

## A note on boundary-layer collision in a curved pipe

By L. TALBOT AND S. J. WONG†

University of California, Berkeley, CA 94720 U.S.A.

(Received 19 January 1982)

Electrochemical measurements of the local wall shear were made along the inner bend of a curved pipe in the entry region, to examine the nature of the secondary-flow boundary-layer collision. Analysis by Stewartson, Cebeci & Chang (1980) predicts a vanishing of the wall shear at the collision point, but without flow reversal. The experimental results are in good agreement with the analytical predictions upstream of the collision point, and its location appears to be predicted accurately. However, downstream of the collision point agreement is poor.

---

In a recent study by Stewartson, Cebeci & Chang (1980) of the boundary-layer development in the entry region of a curved circular pipe a rather curious type of separation was found. On the inner wall of the bend at the location where the secondary (circumferential) flow boundary layers are predicted to collide, the axial component of wall shear stress is found to vanish. However, downstream of this singular point the axial wall shear stress does not change sign, as is normally the case with separation on a line of symmetry, but instead reassumes increasing values of the same sign as upstream of the collision point. A more detailed examination of the structure of the singularity has been made by Stewartson & Simpson (1982), who conclude that the circumferential boundary-layer collision pushes the axial-flow boundary layer away from the wall, causing the displacement thickness to become infinite on the inner bend generator, though remaining finite elsewhere.

A separation of this nature could conceivably result from the coalescence of a saddle point of separation with a nodal point of attachment, as described by Peake & Tobak (1980). However, such separations have apparently not been observed in actual flows. Thus an experimental investigation of the problem seems warranted.

A study of the local distribution of wall shear rate in the entry region of a curved pipe has already been reported (Choi, Talbot & Cornet, 1979; hereinafter referred to as I). The measurements were made by means of the electrochemical limiting-current technique, as described in I. Briefly, in this technique a redox reaction is produced between two nickel electrodes; a small cathode mounted flush with the tube wall at the point under investigation, and a large anode mounted downstream. The measured diffusion-limited current to the cathode is related to the velocity gradient (and hence wall shear stress) at the wall via the L ev eque theory. The redox couple employed in these experiments was a 0.01 molar solution of potassium ferro- and ferricyanide in a 1.0 molar solution of NaOH as supporting electrolyte.

The L ev eque analysis yields for the wall shear rate (or rate of strain)  $\dot{S}$  under limiting current conditions

$$\dot{S} = \frac{1.899(I_L/A_e FC_\infty)^3 l_e}{D^2}, \quad (1)$$

† Present address: Gas Turbine Department, Brown-Boveri & Co., Baden, Switzerland.

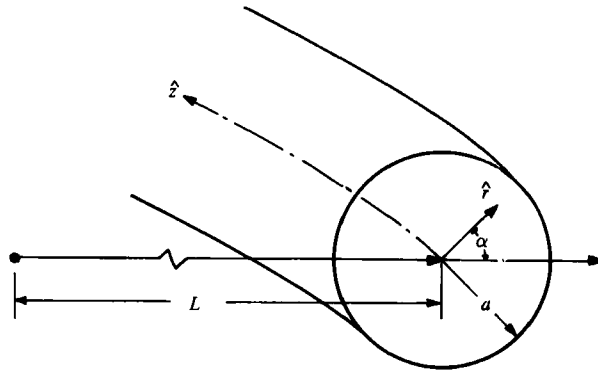


FIGURE 1. Co-ordinate system.

where  $I_L$  is the limiting current,  $A_e$  and  $l_e$  are the dimensional electrode surface area and effective length in the flow direction,  $D$  and  $C_\infty$  are the diffusion coefficient for the ferricyanide ion and its bulk concentration, and  $F$  is Faraday's constant. The theory is expected to be valid if the Péclet number  $Pe = \hat{S}l_e^2/D$  is sufficiently large: measurements by Ackerberg, Patel & Gupta (1978) indicate that  $Pe \gtrsim 400$  is adequate.

The curved pipe used in I was constructed of two semi-circular sections mated together along the  $\alpha = (0, \pi)$  symmetry plane, in the notation of the coordinate system in figure 1. It was therefore not possible in this study to locate electrochemical 'probes' along  $\alpha = \pi$ , and consequently the experiments of I did not provide data on the separation phenomena just described. To rectify this, a new  $180^\circ$  pipe bend was constructed with radius-to-curvature ratio  $\delta = a/L = \frac{1}{2}$ , the two halves of which mated along the  $\alpha = (\frac{1}{2}\pi, \frac{3}{2}\pi)$  plane. The flush-mounted nickel cathodes of diameter  $\hat{d}_e = 1.587 \times 10^{-1}$  cm were installed at different axial locations  $z = \hat{z}/(aL)^{\frac{1}{2}}$  along  $\alpha = \pi$ , where  $\hat{z}$  is the dimensional distance along the pipe centreline measured from the entrance, and  $a$  ( $= 1.905$  cm) is the pipe cross-sectional radius. The spacing of the probes was selected so as to provide as much resolution as possible in the vicinity of the predicted location of the separation point, and farther downstream the locations were chosen to be the same as those employed in I. The construction and mounting of the probes was identical to that of I. Table 1 lists the locations of the probes.

The experimental procedures employed were the same as described in I. Prior to making measurements in the curved pipe, the probes were installed and tested in a straight tube under conditions of fully-developed Poiseuille flow, for which the wall shear rate is

$$\hat{S}_P = \frac{2\nu R}{a^2}, \quad (2)$$

where  $\nu$  is the fluid kinematic viscosity and  $R = 2\hat{W}_0 a/\nu$  is the Reynolds number based on the mean axial velocity  $\hat{W}_0$  and tube diameter  $2a$ .

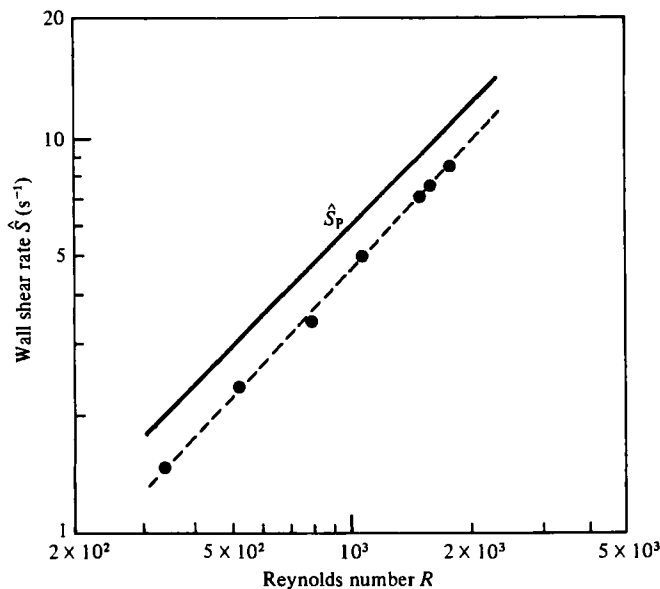
Figure 2 shows the results of the calibration experiments as interpreted by the Lévêque analysis, using for the effective length of a circular electrode of diameter  $\hat{d}_e$  the value

$$l_e = 0.8136\hat{d}_e \quad (3)$$

given by Mizushima (1971) and employing the electrolyte property values

Probe	$z$
1	0.38
2	0.66
3	0.96
4	1.22
5	1.49
6	2.00
7	2.77
8	3.50
9	5.08
10	7.39

TABLE 1. Probe locations

FIGURE 2. Probe calibration of wall shear  $\hat{S}$  vs. Reynolds number: ----, data fit; —,  $\hat{S}_P$ .

$\rho = 1.043 \times 10^3 \text{ kg/m}^3$ ,  $\nu = 1.064 \times 10^{-6} \text{ m}^2/\text{s}$  and  $D = 6.326 \times 10^{-10} \text{ m}^2/\text{s}$ . It can be seen that the calibration data for  $\hat{S}$  vary linearly with Reynolds number, as they should, but fall about 15% below the theoretical Poiseuille value. A similar though somewhat smaller discrepancy was observed in I, and also by Ackerberg *et al.* Probably the discrepancy was due to some residual poisoning of the electrodes, although they were cleaned mechanically and treated cathodically under hydrogen evolution conditions prior to each experimental run. Axial and lateral diffusion effects are not believed to have been of importance, since for all these data  $Pe > 4 \times 10^3$ , and in any case, such effects result in an increase in mass transfer over the Lévêque value.

Data were obtained in the curved pipe for Dean numbers  $\kappa = R\delta^{\frac{1}{2}}$  ranging from 188 to 1622. To compare with the results of Stewartson *et al.*, the data are presented in figure 3 in terms of the non-dimensional wall velocity gradients  $S_z(\pi, z) = [(\partial w / \partial \eta)_{\eta=0}]_{\pi, z}$  versus the non-dimensional axis distance  $z$ . The axial velocity  $w$  is normalized by the bulk velocity  $W_0$ , and  $\eta = (1 - r/a)(\frac{1}{2}\kappa)^{\frac{1}{2}}$  is a magnified dimensionless co-ordinate that arises in the analysis of high-Dean-number boundary-

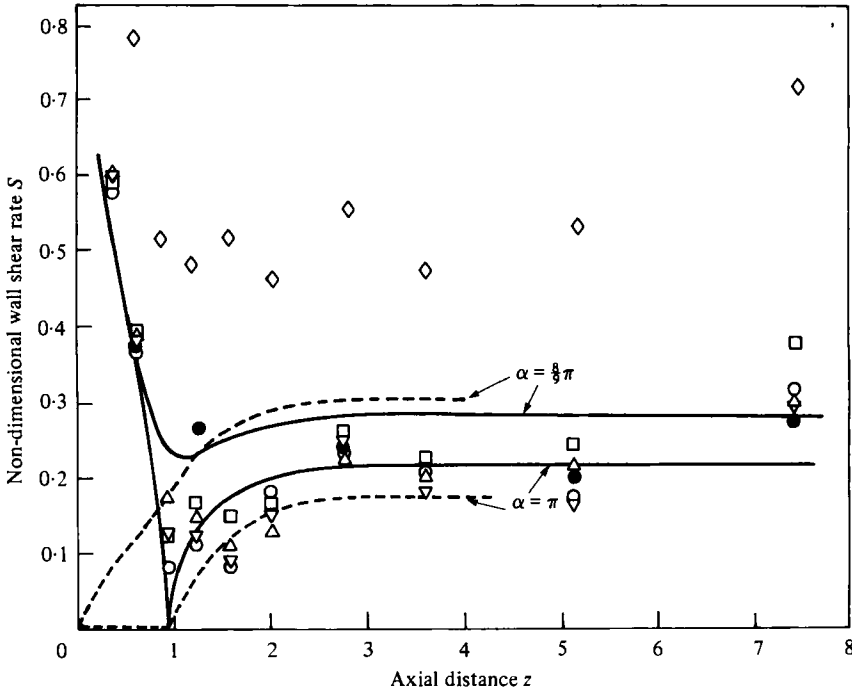


FIGURE 3. Experimental results and comparison with analytical predictions. Present results for  $S_z(\pi, z)$ :  $\diamond$ ,  $\kappa = 188$ ;  $\square$ , 643;  $\triangle$ , 949;  $\nabla$ , 1355;  $\circ$ , 1622. Choi *et al.* (1979):  $\bullet$ ,  $\kappa = 643$ ,  $S(\frac{3}{8}\pi, z)$ . Stewartson *et al.* (1980): —,  $S_z$ ; - - - - - ,  $S_x$ .

layer flow. Shown for comparison are the theoretical predictions for  $S_z$ , for  $\alpha = \frac{3}{8}\pi$  and  $\alpha = \pi$ , the latter curve exhibiting the vanishing of the wall shear at  $z = z_s = 0.943$ .

The data for  $z < z_s$  follow very well the theoretical prediction at all but the lowest Dean number  $\kappa = 188$ . There is indeed a minimum in  $S_z(\pi, z)$  recorded by the probe located at  $z = 0.96$ , very close to the predicted separation point at  $z_s = 0.943$ , and although  $S$  does not vanish there the trend is toward decreasing values of  $S_z$  with increasing values of  $\kappa$ . Of course, if  $S$  did in fact vanish at  $z_s$ , our measurements would not record a zero value because of the averaging effect due to the finite size of the probes.

Since the analysis of Stewartson *et al.* is an asymptotic analysis in the limit  $\kappa \gg 1$ , in which terms of order  $\kappa^{-\frac{1}{2}}$  and smaller are neglected, the trend of decreasing  $S_z(\pi, z_s)$  with increasing  $\kappa$  is consistent with an approach to an asymptotic limit  $S_z(\pi, z_s) = 0$  as  $\kappa \rightarrow \infty$ , although it seems to us unlikely that in a flow with finite Dean number an actual separation point with  $S = 0$  will occur.

Downstream of  $z = z_s$ , the agreement between theory and experiment is less good. Whereas the analysis predicts a rapid increase in  $S_z(\pi, z)$  towards an asymptotic value for  $z \gtrsim 3$ , the experimental values of  $S_z(\pi, z)$  at all Dean numbers remain fairly constant at their minimum values in the region  $z_s \lesssim z \lesssim 2$ , and with the exception of the  $\kappa = 188$  data, are generally lower than the theoretical prediction. In the region  $2 \lesssim z \lesssim 7$  for all Dean numbers there is a non-monotonic variation of  $S_z(\pi, z)$  which, as discussed in I, is most likely associated with a vortex structure imbedded within the Dean-type secondary motion. Here the values of  $S_z(\pi, z)$  appear to agree

reasonably well with the theoretical prediction but this is undoubtedly fortuitous, for reasons to be discussed.

Data for  $S(\frac{2}{3}\pi, z)$  obtained in I are also plotted in figure 3. Except in the immediate vicinity of  $z_s$ , these data agree rather well with the present data for  $S_z(\pi, z)$ . We note that the electrochemical method measures the resultant of the axial and secondary flow wall shear rates, so that

$$S = (S_z^2 + S_\alpha^2)^{\frac{1}{2}},$$

where  $S_\alpha = (\partial v / \partial \eta)_{\eta=0}$ ,  $v$  being the non-dimensional circumferential flow velocity given by  $\hat{V} / \hat{W}_0 \delta^{\frac{1}{2}}$ . The general agreement in the region  $z > z_s$  between the data for  $S_z(\pi, z)$  and  $S(\frac{2}{3}\pi, z)$  for the higher Dean numbers would indicate that  $S_z(\frac{2}{3}\pi, z) \gg S_\alpha(\frac{2}{3}\pi, z)$  in this region, which is counter to the predictions of Stewartson *et al.* as seen in figure 3. This in turn suggests that the secondary-flow boundary layer has already separated at a value of  $\alpha \leq \frac{2}{3}\pi$ , which is consistent with the prediction of Yao & Berger (1975), although comparisons with the results of Yao & Berger must be made with caution, since they predict the separation to persist throughout the fully-developed flow, which is at variance with the numerical results of Collins & Dennis (1975). The separation flow pattern envisioned is similar to that considered by Smith & Duck (1977) in the case of two colliding wall jets, although the mechanisms responsible for the separation are clearly different; in the Smith & Duck model the pressure field is induced by the jet interaction, whereas in the present case the pressure field is largely due to the curvature of the axial flow.

The fact that the solution obtained by Stewartson *et al.* agrees well with experiment for  $z < z_s$ , but does not for  $z > z_s$ , is of considerable interest. In the method they employed, the equation governing the flow field on  $\alpha = \pi$  could be solved independently of the rest of the flow field up to  $z = z_s$ , and it appears that the analysis in this region gives an accurate description of the evolution of the wall shear and the location of the circumferential boundary-layer collision. However, for  $z > z_s$  the flow at  $\alpha = \pi$  was calculated by numerical integration of the equations in the circumferential direction starting at  $\alpha = 0$ , using the Keller box method. The conventional symmetry condition on the circumferential velocity could therefore not be applied, and in fact it was found that for  $z > z_s$ ,  $S_\alpha$  (and  $v$  as well) was finite at  $\alpha = \pi$ , as seen in figure 3. Professor Stewartson (private communication) has suggested that this may indicate that the boundary-layer collision is essentially inviscid in character, and that a sub-boundary layer must be set up beneath it which separates at  $\alpha = \pi$ . The work of Stewartson & Simpson lends support to this idea, but the theory is thus far unable to shed light on the nature of the flow downstream of  $z_s$ . Clearly, the nature of the boundary-layer collision that occurs in a curved pipe is far from being understood.

This work was supported by the National Science Foundation under Grant MEA 77-23934. The authors acknowledge helpful discussions with Professor Stanley A. Berger, and the assistance of Dr S. Choi in the early stages of the experiment.

#### REFERENCES

- ACKERBERG, R. C., PATEL, R. D. & GUPTA, S. K. 1978 *J. Fluid Mech.* **86**, 49–65.  
 CHOI, U. S., TALBOT, L. & CORNET, I. 1979 *J. Fluid Mech.* **93**, 465–489.  
 COLLINS, W. M. & DENNIS, S. C. R. 1975 *Q. J. Mech. Appl. Math.* **28**, 133–156.

- MIZUSHINA, T. 1971 *Adv. Heat Transfer* **7**, 87–161.
- PEAKE, D. J. & TOBAK, M. 1980 Three-dimensional interactions and vortical flows with emphasis on high speeds. *AGARDograph* no. 252.
- SMITH, F. T. & DUCK, P. W. 1977 *Q. J. Mech. Appl. Math.* **30**, 143–156.
- STEWARTSON, K., CEBECI, T. & CHANG, K. C. 1980 *Q. J. Mech. Appl. Math.* **33**, 59–75.
- STEWARTSON, K. & SIMPSON, C. J. 1982 *Q. J. Mech. Appl. Math.* **35**, 291–304.
- YAO, L. S. & BERGER, S. A. 1975 *J. Fluid Mech.* **67**, 177–196.